International Journal of Electronics and Instrumentation Engineering (IJEIE)
Volume 3, Issue 1, January-June 2025, pp. 7-23, Article ID: IJEIE_03_01_002
Available online at https://iaeme.com/Home/issue/IJEIE?Volume=3&Issue=1
Journal ID: 2416-1724; DOI: https://doi.org/10.34218/IJEIE_03_01_002

DEVELOPMENT OF MOO$_3$ AND CU DOPED MOO$_3$ NANOPARTICLES AND ITS COMPUTATIONAL ANALYSIS FOR LITHIUM ION BATTERY AS ANODE ELECTRODE MATERIALS FOR ENERGY STORAGE APPLICATIONS

Harini R [1,2], Sunil T D[1*], Kunal Roy[3], Dinesh Rangappa[3], G. Nagaraju[4]

[1] Department of Electronics and Communication Engineering, Sri Siddaratha Institute of Technology, Tumakuru, Karnataka 572105, India.

[2] Department of Electronics and Communication, Government Polytechnic, Hiriyuru, Karnataka 577599, India.

[3] Department of Applied Sciences (Nanotechnology), Centre for Post-Graduate Studies, Visvesvaraya Technological University, Muddenahalli 562101, India.

[4] Energy Materials Research Laboratory, Department of Chemistry, Siddaganga Institute of Technology, Tumakuru, Karnataka 572103, India.

ABSTRACT

The Molybdenum trioxide Nanoparticles (MoO_3 NPs) and Cu doped MoO_3 NPs have been successfully fabricated by green combustion methodolgy using Terminalia catappa (Indian almond) tree leaves powder. The X-ray diffraction (XRD), Fourier transform infrared spectroscopic (FTIR), scanning electron microscopic (SEM), Photoluminescence and Ultraviolet-Visible diffuse reflectance spectroscopic (UV-DRS) *techniques were used to characterize the MoO_3 nanoparticles. The XRD patterns of synthesized material shows orthorhombic phase. The Scherer's method was adopted to find the crystallite size of the synthesized material. The Cu doped MoO_3 shows increased specific capacity, better cyclic performance and rate performance than MoO_3 at room temperature. The electrochemical of Cu doped MoO_3 exhibited higher specific capacity 410 $mAhg^{-1}$ than MoO_3, while its specific capacity is 303 $mAhg^{-1}$.*

Keywords: Molybdenum oxide, Green synthesis, Terminalia catappa, Doped Nanoparticles.

Cite this Article: Harini R, Sunil T D, Kunal Roy, Dinesh Rangappa, G. Nagaraju. (2025). Development of MoO_3 and Cu doped MoO_3 Nanoparticles and its computational analysis for Lithium ion battery as anode electrode materials for energy storage applications. *International Journal of Electronics and Instrumentation Engineering (IJEIE)*, 3(1), 7–23.

https://iaeme.com/MasterAdmin/Journal_uploads/IJEIE/VOLUME_3_ISSUE_1/IJEIE_03_01_002.pdf

1.0. Introduction

Energy plays a vital importance in our everyday life, has it is accepted as the one major resource for the many activities. There are wide new and advanced technology evolved with increasing demand for energy like Lithium (li)-ion batteries, light-emitting diode (LED), solar cell, fuel cells, and ultra-capacitor were used to save the energy. According to the studies li-ion batteries shows high energy and high power density [1]. Also li-ion batteries are extensively used in home electronics, automotive applications, mobiles, laptops because as it posses long cyclic life, high efficiency, high volumetric and gravimetric energy. Hence li-ion batteries are widely used as powerful and future candidate for energy storage application [2]. As a result, li-ion battery technology is an open and challenged title in several scientific fields. The performance of li-ion battery depends on design and fabrication of electrode material and also its electrochemical characteristics. Nanotechnology tremendously influence for cost reduction technique, generation of efficient energy, transmission and storage technique. The production of nanomaterials and nanostructures energetically use for producing a advanced devices with better efficiency, lower cost, and very low energy demand in several applications like solar photovoltaic systems, solar thermal systems, hydrogen production, and energy saving technologies [3].

The present trend is also concerned with low cost of production compared to old and other technologies. To achieve better efficiency with low manufacturing cost, the high priority should be given to the nanotechnology. Nanomaterial is the important cornerstones of Nano science. Nanostructure science and technology having a broad research and development integrative activity that has been growing from few past years[4]. In recent years Nano materials has become one of the most important and exciting fields of research in physics, chemistry, medicine, engineering and technology fields [5].The usage of Nano materials are enormous as energy storage device such as fuel cell detection of threats in defense, navy, drug delivery and water purification [6]. Currently there are one dimensional (1D) and two dimensional (2D) nanomaterials utilized for energy storage products due to its good life period and high efficiency [7]. Various transition metal oxide nanomaterials shows good electrochemical properties for li-ion batteries such as MoO_3[8],MnO_2[9], RuO_2[10], NiO and Fe_2O_3[11, 12]. Among them MoO_3 is very attracted transition metal oxide with fascinating electrode material properties in li-ion battery. It has more advantageous properties like low cost, huge abundance, good structural stability, layered structure, less toxic, high theoretical capacity [13, 14].

Materials like Molybdenum have been studied alternative for toxic and rare elements used in many catalyst, however they may present poor recyclability or require harsh conditions to be useful[15]. Transition metal oxides comprises a large family of materials exhibiting a varieties of interesting properties, that are attractive for application of lithium ion battery, catalyst, electrochemical sensors[16]. Molybdenum is used as a nanomaterial due to its unique properties and potential applications at the Nano scale and it is also utilized in nanotechnology, Molybdenum is an important refractory materials. It has very high melting point, high electrical conductivity [17]. A layered oxygen deficient orthorhombic MoO_3 NPs (alpha-phase) on thermal photo and electrical excitations, it is showed electro chromic and photochromic property which make MoO_3 NPs amiable for winder application in lithium ion battery, gas sensors and photolysis[18].On this account photo catalysis is a widely utilized technique to eliminate pollutants from water bodies with sunlight as a source in mind[19].

Doping with transition metal ion is another methodology to vary the properties of functional materials. Because of bonding of electronic states and tendency to occupy the sites in the crystalline structure, MoO_3 NPs with doping metal ion may be projecting new phenomena not found in individuals materials [20].Cu doping can effectively improve the capacitive performance and rate capability. Which may be imply new insights into establishing a doping model[21]. Cu doping refers to the process of incorporating copper (Cu) atoms into the structure of a material, typically a metal oxide, to modify its properties. In the context of capacitive performances and also rate capability, Cu doping has been found to be beneficial in several ways[22].

Several methods available to fabricate MoO_3 NPs are hydrothermal, co-precipitation, sol-gel[23, 24] , etc. The above said methods requires high cost substrates, very tedious procedures, well sophisticated equipment, good and stable experimental conditions, controlled conditions, etc. The combustion method is widely adopted because of a simple, versatile and synthesis method requires less time and offer mass quantity for further usage [25]. And the production of nanomaterials by adopting combustion method produces uniform distribution and form a material with reduced particle size[26]. Also, the importance of combustible fuel is having equal important for the liberation of high energy to produce soft mass of nanomaterials in the combustion method. [27].

Researchers have prepared MoO_3 by using green fuel. The chemicals used for the synthesis of nanoparticles and stabilization are dangerous and lead to toxic by-products. Also the chemicals used for the synthesis are too expensive and the use of toxic chemicals which are very dangerous to the health and environment [28]. Hence to avoid this problems, researchers are using environment-friendly fuels to synthesis MoO_3 NPs[29].

2.0. Experimental details:

2.1. Fuel extraction

The *Terminalia catappa* (Indian almond) tree leaves were freshly collected, cleaned with water to remove the impurities and dried for 20 days at room temperature. Dried leaves were roughly crushed into small pieces and then finely powdered using grinder. The finely grinded powder was filtered and stored at room temperature. The same powder was used for synthesis of nanostructued MoO_3 NPs as fuel.

2.2 Materials

Ammonium heptamolybdate tetrahydrate $[(NH_4)_6Mo_7O_{24}.4H_2O]$ and Cupric nitrate trihydarte $[Cu\ (NO)_3.3H_2O]$ was purchased from SDFCL Chemicals and green fuel *Terminalia catappa* (Indian almond) tree leaves powder.

2.3 Preparation

Synthesis of MoO_3 Nanoparticles by combustion method. Precursors are Ammonium heptamolybdate tetrahydrate $[(NH_4)_6Mo_7O_{24}.4H_2O]$ and finely powdered *Terminalia catappa* (Indian almond) tree leaves powder. Stoichiometric ratio of both precursors and fuel are 1:0.25, 1:0.5, 1:1 and 1:1.5 were taken in a silica crucible having a water about 10 ml .The content were stirred well and introduced into the preheated 500^o temperature asserted muffle furnace. Combustion process was concluded in 10 minutes with the formation of black coloured MoO_3 as a product and then it introduced to 3 hours for calcination to remove the impurity after it a yellowish MoO_3 as a product.

Similar procedure was followed for synthesizing Cu doped MoO_3. During the reaction cupric nitrate [$Cu(NO_3)_2.2H_2O$ was added along with a Mo. The synthesis was carried out for 5 different percent's are 2%Cu, 4%Cu, 6%Cu, 8%Cu and 10%Cu MoO_3 NPs.

2.4 Characterization:

The principle characterization of MoO_3 NPs was performed using various techniques to understand its crystallinity, phase, purity, bonding, optical properties, and microstructure. The specific characterization methods used are as follows:

X-ray Diffraction (XRD) Analysis: Rigaku Smart Lab X-ray diffractometer CuKα (1.541 Å) irradiation to the MoO_3 NPs sample at room temperature. To study the diffraction pattern produced by the sample, which provides information about its crystal structure and composition.

Fourier Transform Infrared Spectroscopy (FT-IR): Metal to metal bonding and the bonding of MoO_3 NPs and its oxides were examined using a Bruker-Alpha FT-IR spectrophotometer. It measures the absorption and transmission of infrared light by the sample, allowing the identification of functional groups and chemical bonds present.

UV-Visible Diffuse Reflectance Spectroscopy (UV-Vis DRS): The optical properties of MoO_3 NPs were characterized using a LAB INDIA UV 3092 spectrophotometer in reflectance mode. It measures the absorption and reflectance of light across a range of wavelengths, providing information about the energy bandgap and electronic transitions in the material.

Photoluminescence Spectroscopy: The photoluminescence properties of MoO_3 NPs were studied using a Cary Eclipse fluorescence spectrophotometer by Agilent Technologies. This technique involves illuminating the sample with light and measuring the emitted fluorescence, which can provide insights into the energy levels and excitonic behavior of the material by employing these characterization techniques, researchers can gain a comprehensive understanding of the MoO3 sample's properties and behavior, including its crystal structure, chemical bonds, optical response, and surface morphology.

Scanning Electron Microscopy (SEM): The microstructure and structural configuration of MoO_3 NPs were examined using a Hitachi TM 300 scanning electron microscope. SEM produces high-resolution images of the sample's surface by scanning it with a focused beam of electrons, enabling visualization of the morphology, grain size, and surface features of the material.

3.0. Results and discussion

3.1. XRD Studies

The product of pure MoO_3 NPs and Cu doped MoO_3 NPs was subjected to XRD analysis was used with 2θ ranging from 10º to 80º. The XRD analysis confirmed that the obtained product was pure MoO_3 nanoparticles using JCPDS number 01-076-1003. The fig (1) shows that the maximum peak intensity XRD peaks for pure MoO_3 observed at 27.32º and corresponding diffraction are (021). High crystallanity and high intensity peak was observed for the sample 1:0.5 MoO_3 NPs compared to other synthesized samples. As the crystalline size decreases quantum confinement effect increases which reduces the stability and increases the strain, thereby increased catalytic activity[19]. The XRD analysis revealed that the MoO_3 nanoparticle had an orthorhombic structure[20].

The XRD analysis confirmed that the obtained product was copper doped MoO_3 nanoparticles using JCPDS number, when the peak values are compared they matched with JDPDS card number 01-1-1241. The peak broadening was observed on increasing Cu concentration (Figure1 (b)) due to the contribution of crystalline size. The crystallite size was found to be decrease with the increase in dopant concentration which is due to the difference in ionic radius between Cu and Mo ions[21]. Lattice parameters values are found to pure MoO_3 a = 3.9628Å, b = 13.8550Å and c = 3.6964Å and for Cu doped is a= 3.6077Å. From the debye-scherrer equation, the average crystallite size of pure and copper doped MoO_3 were estimated to be 41.98nm and 44.39nm respectively. The debye-scherrer formula is

$$D = \frac{K\lambda}{\beta COS\theta}$$

Where, **D** is the average grain size or crystallite size **λ** signifies the wavelength of the X –ray, **k** is the crystallite shape factor **β** is the width at half maximum and **θ** is the Bragg's diffracting angle.

JCPDS No 01-076-1003 and 1-1241.

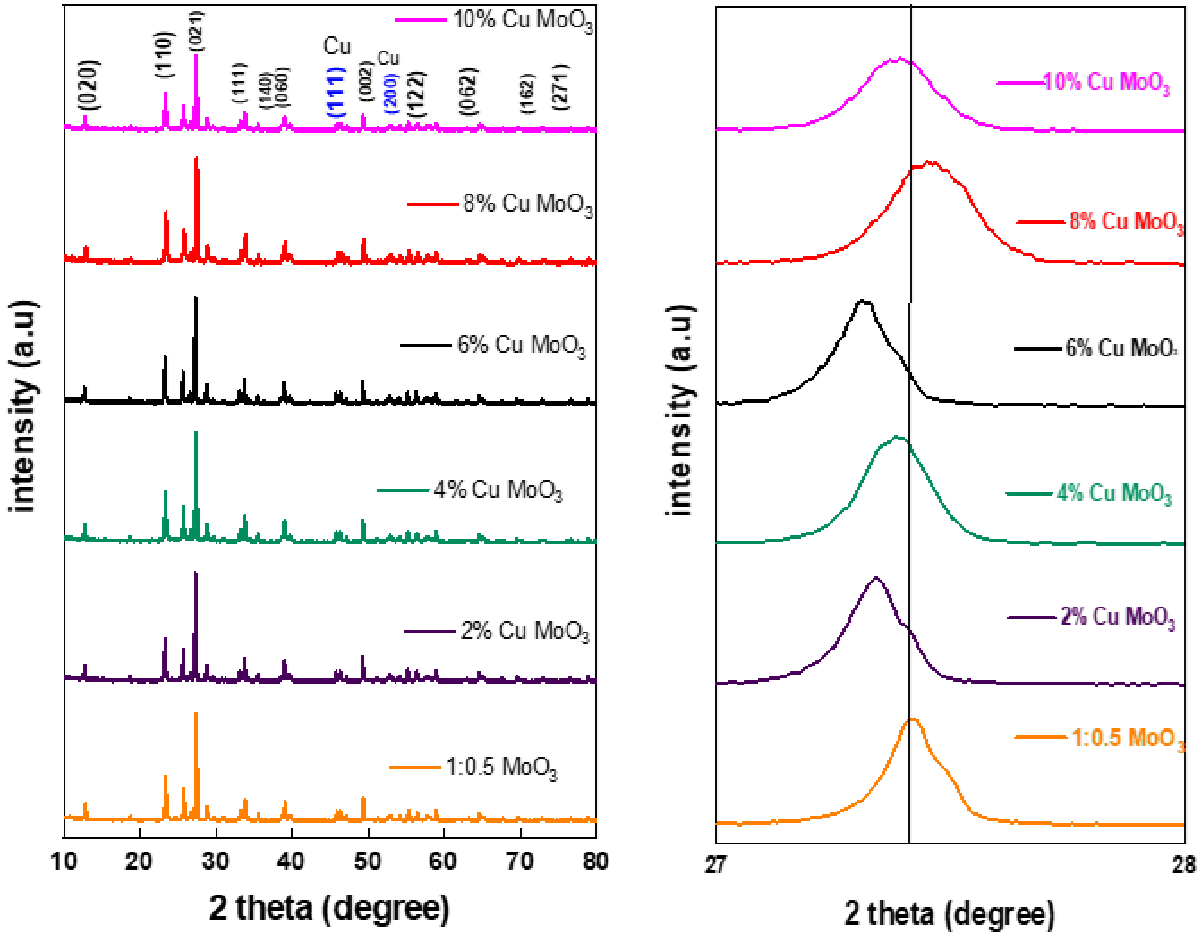

Fig 1(a): XRD patterns of Pure and Cu doped MoO_3 Fig 1(*b*): XRD peak broadening of pure and copper doped MoO_3

3.2 FTIR Studies:

The Fourier transform infrared spectroscopy (FT-IR) analysis is carried out using the instrument BRUKER ALPHA spectrophotometer. FTIR is important spectroscopic tools to identify the metal oxygen vibration and impurities present in the prepared samples.The FT-IR spectra of pure and Cu doped MoO_3 NPs. All the spectra were recorded in the range of wave number 400-4000 cm^{-1}.Cu doped MoO_3 NPs spectra show similar spectra peaks corresponding to characteristic peaks of pure MoO_3. The vibration spectra (Figure. 2(a)) is drawn from 400 to 4000 cm^{-1} and exhibits the transmittance peaks at 578, 856 and 991 $cm^{-1.}$ indicates the presence of Mo-O bonds in the as-prepared materials[22, 23]. The peak at 578 cm^{-1} shows bending non planar vibration of Mo-O. The peak at 856 cm^{-1} indicates the

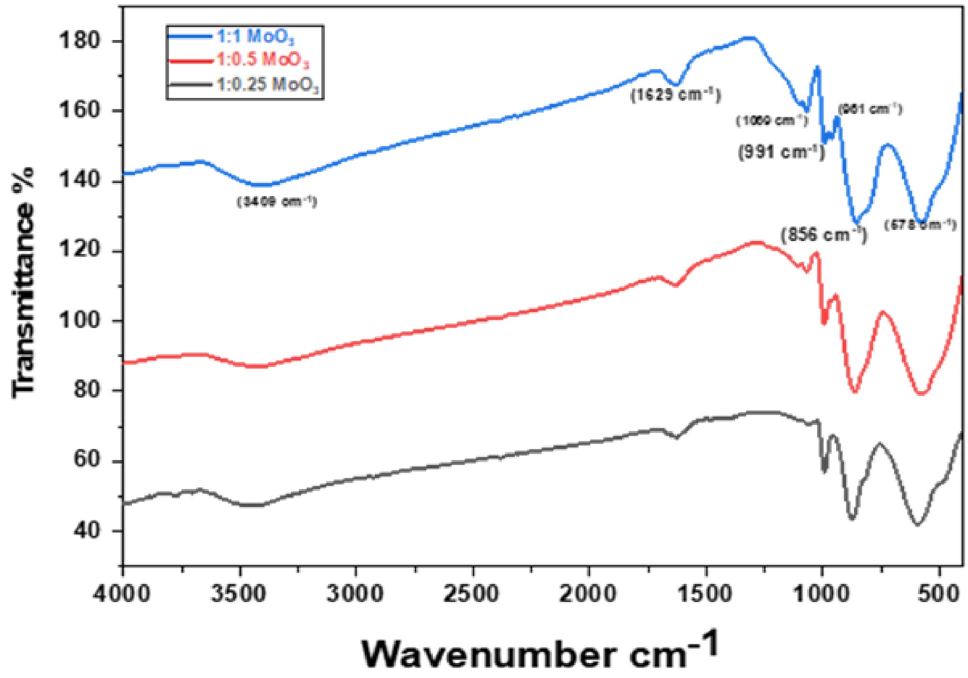

Fig.2 FTIR transmission spectra for pure MoO_3

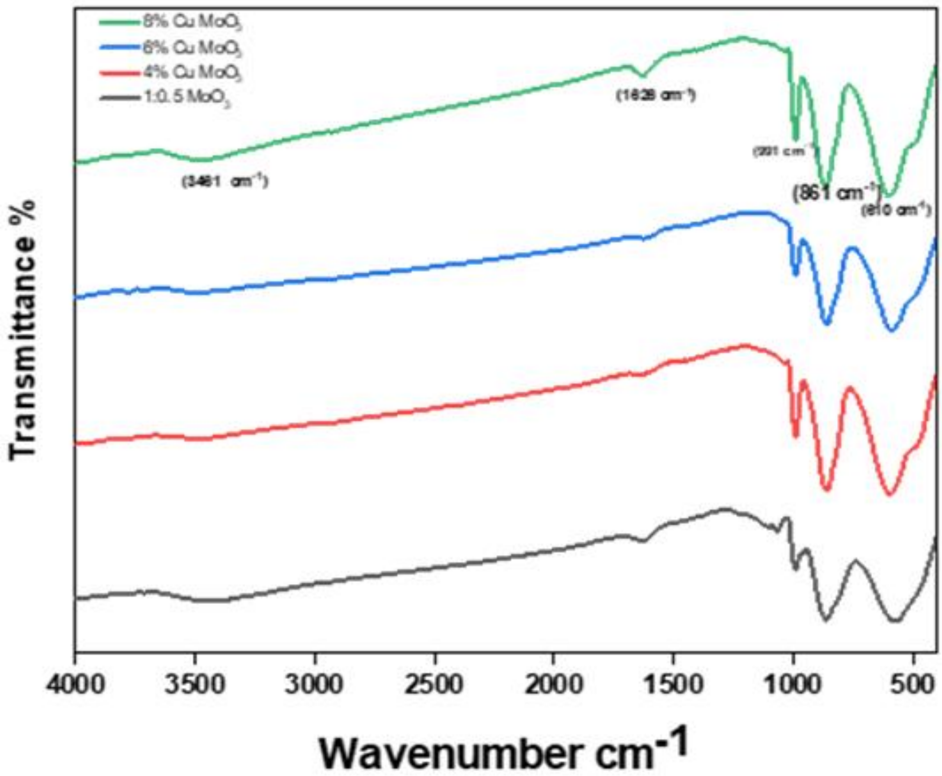

Fig.2(a). FTIR transmittance spectra for Cu doped MoO_3

Presence of oxygen atom sandwiched between two molybdenum atom as Mo^{6+} and the presence of terminal Mo=O is appeared at 991 cm^{-1} [24]. All these vibrations of Molybdenum to oxygen indicates the existence of materials in α-MoO_3 phase. The presence organic moiety from the fuel is observed at 1629 cm^{-1} corresponds to the existence of C=C stretching planar vibration[25]. It is noticed that as the fuel ratio (carbon content) increases, the peaks corresponds to C=C also increases. Broad peak around 3409 cm^{-1} indicates the presence of O-H non planar stretching vibrations of water. Presence of water is observed which may be the moisture absorption during pallet preparation.

3.3 Photoluminescence studies:

Photoluminescence studies of MoO_3 NPs and Cu doped MoO_3 NPs provide an information about the presence of defects, certain kinds of vacancies, charge transfer incidence between the donor and acceptor atoms, and charge recombination properties. Fig. **3a** and **3b** represent the emission and excitation spectra of the prepared NPs, with an excitation wavelength of 324 nm, emission spectra at wavelength of 486 nm. Fig. **4a** and **4b** represent emission and excitation spectra of Cu doped MoO_3 NPs, with excitation wavelength at 330nm, and emission spectra found at 493nm. An intense peak found in the PL spectra corresponds to pure MoO_3 NPs and Cu doped NPs. The emission peaks at 486 nm and 493nm are due to the surface state emissions and the presence of O_2 vacancies thus, it induces the recombination of trapped electrons and holes resulting from the loose bonds in the MoO_3 NPs and Cu doped NPs respectively[26]. A bare MoO_3 NPs encloses a number of point defects called oxygen vacancies. It serves as a location for recombination of electrons (e) and holes (h), hence the highest PL intensity. The quenching of the PL intensity is due to the occupation of the oxygen vacancies by the doped material, which hampers the recombination rate. Also, lattice distortion occurs at the highest doping concentration; this induces nonradiative emission and reduces the PL intensity.

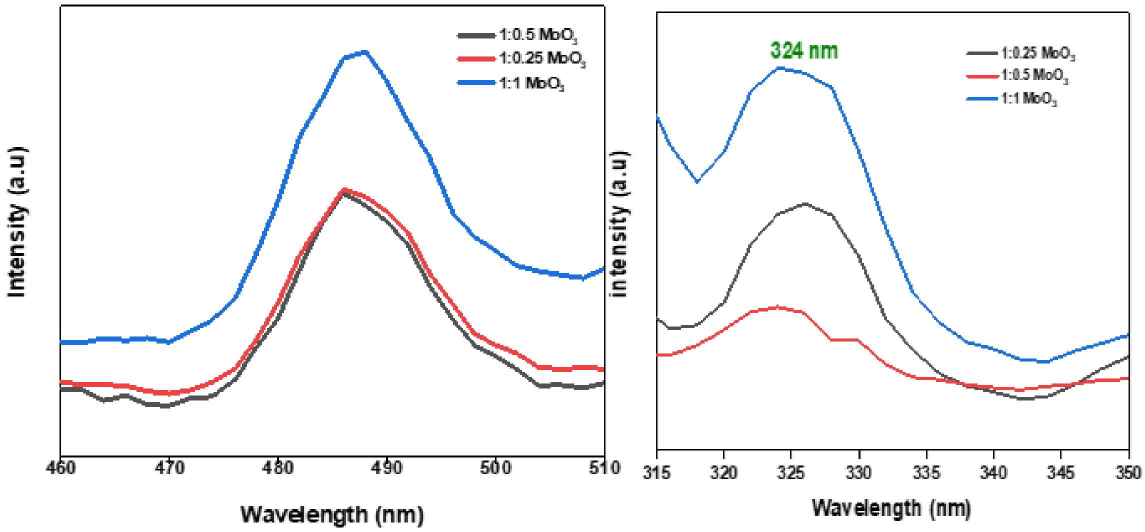

Fig .3(a). Emission spectra of pure MoO_3 NP s (b).Excitation spectra of pure MoO_3 NPs

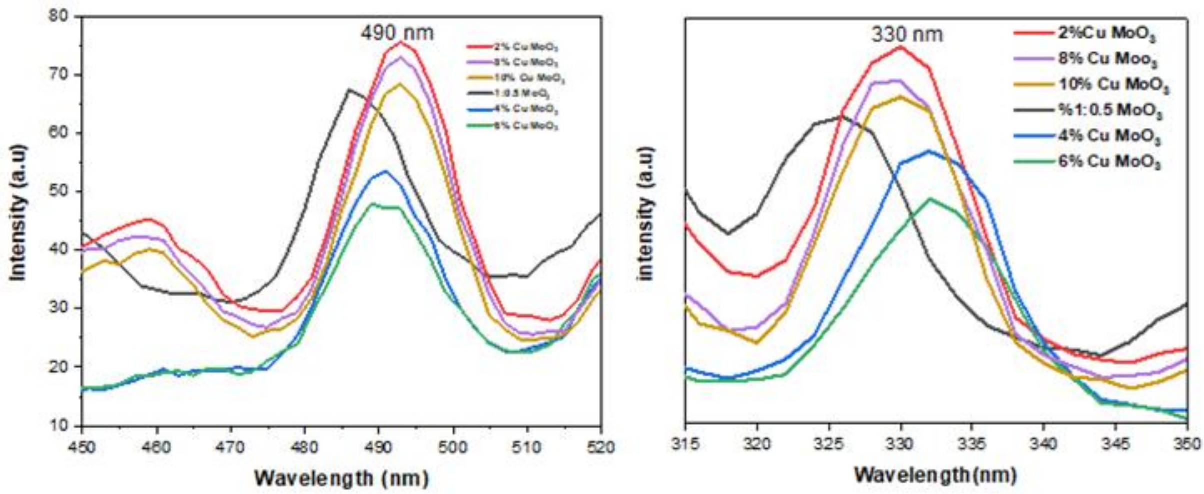

Fig.4 (a) Emission spectra of Cu doped MoO_3 NPs and Fig.4 (b). Excitation spectra of Cu doped MoO_3 NPs

3.4 UV- Visible DRS studies:

The optical properties of the synthesized MoO_3 NPs was estimated by using DRS spectra and obtained spectra was shown in the fig 5. The spectra was obtained by plotting F(R) on y axis and wavelength on the x axis.

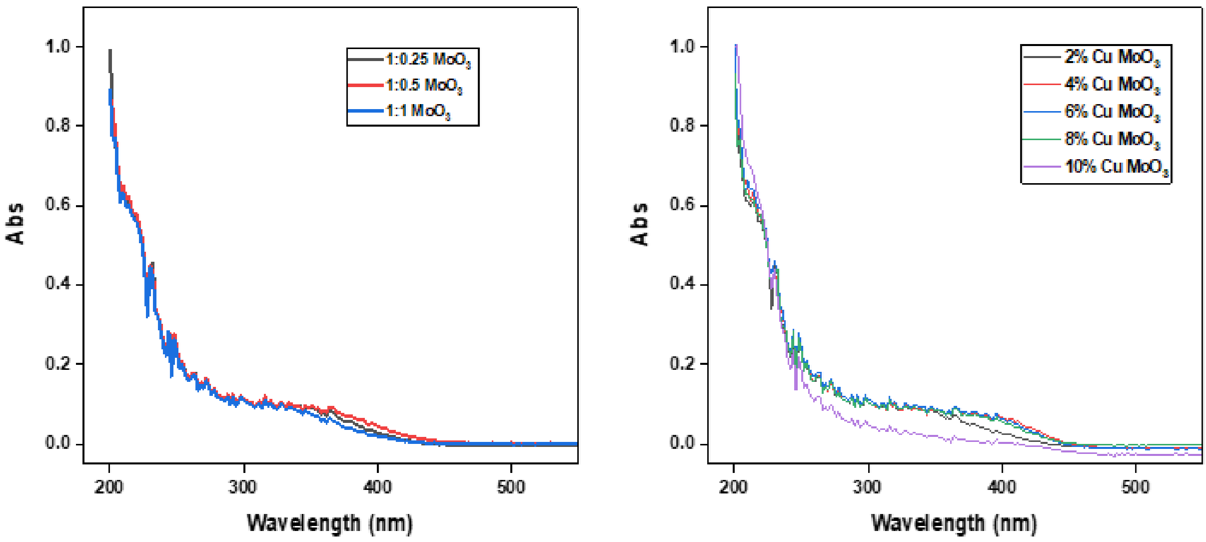

Fig.5: UV- Visible DRS of Pure MoO_3 and Cu doped MoO_3

3.5 SEM studies:

Fig **6** shows the Shows the SEM micrographs of pure MoO_3 NPs and Cu doped MoO_3 NPs which is used to capture surface morphology. SEM images of pure MoO_3 NPs clearly shows porous composite flaky structure and Cu doped MoO_3 NPs shows trapezoidal prism structure.

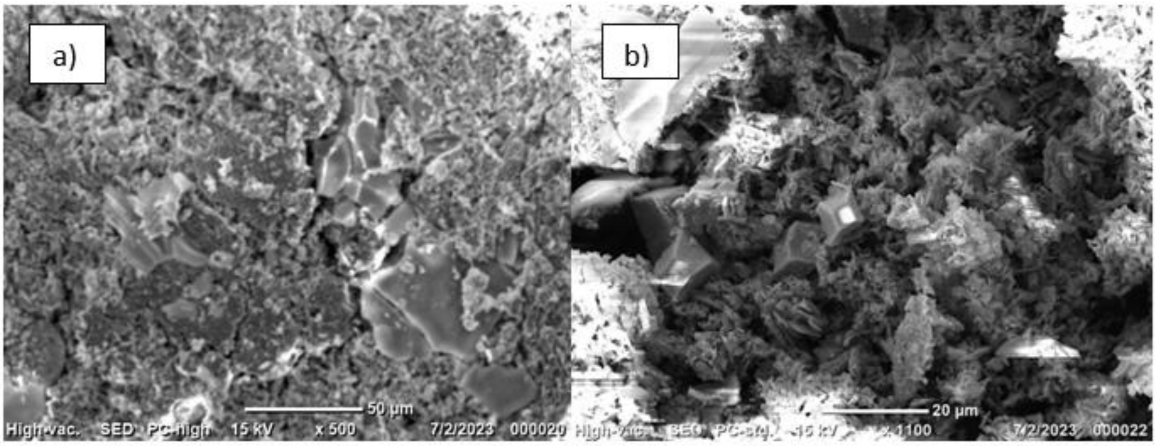

Fig.6: SEM images of a) Pure MoO_3 b) Cu doped MoO_3

3.6. TEM Studies

The TEM images show distinct morphological differences between pure and Cu-doped MoO_3. Pure MoO_3 (Fig. 7a) consists of mostly spherical, agglomerated nanoparticles. These particles are uniformly distributed and nanoscale in size (~50 nm). Cu-doped MoO_3 (Fig. 7b) shows rod-like and elongated structures. This morphological change suggests Cu doping alters growth kinetics. Such transformation may improve surface area and functional properties.

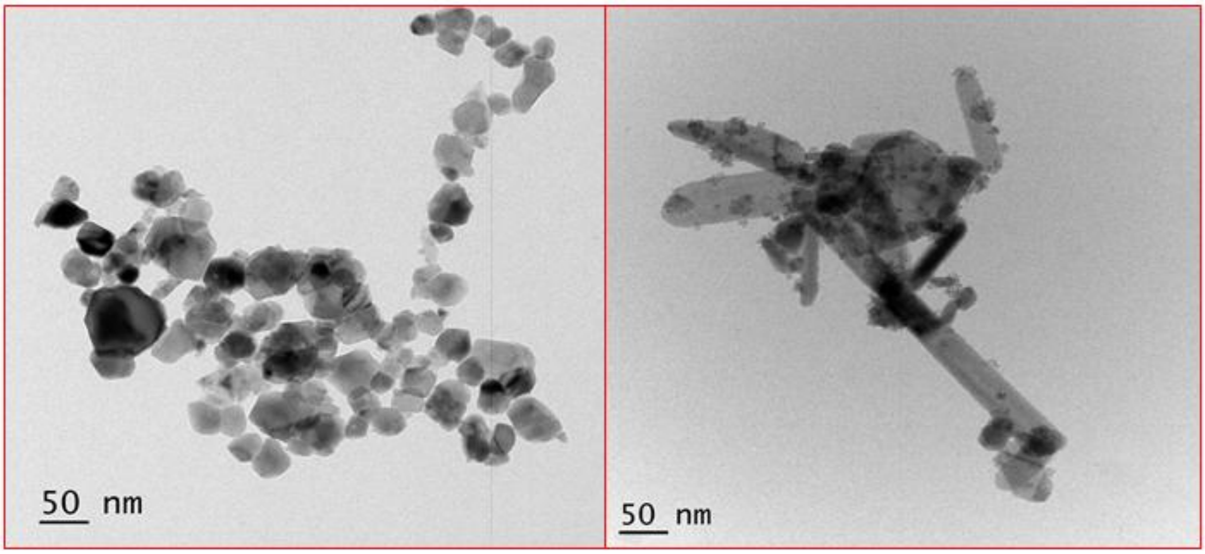

Fig.7: TEM images of a) Pure MoO_3 b) Cu doped MoO_3

4.0. Electrochemical characterization

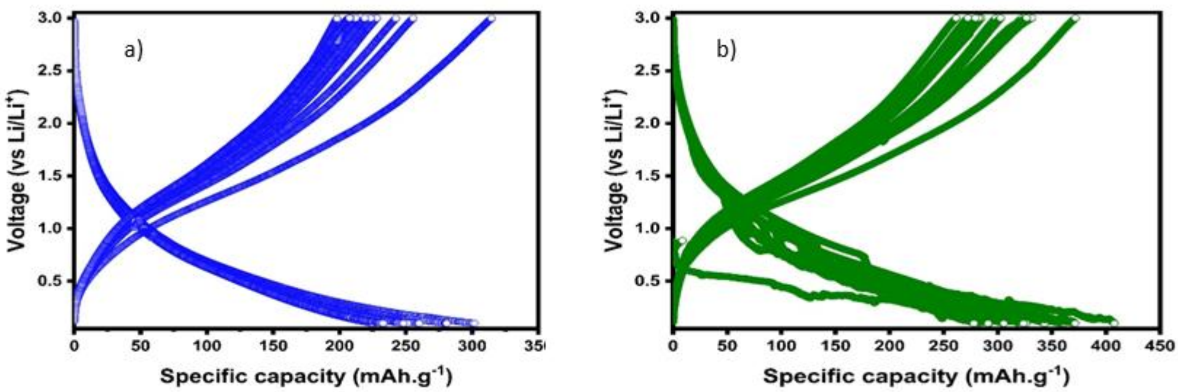

Fig.8: Charge-Discharge profile of a) Pure MoO_3 b) Cu doped MoO_3

Figure 8(a) presents the Galvonastatic charge-discharge profile of pure MoO_3 nanoparticles for 100 cycles and its first charge-discharge capacities are found to be 310 mAh/g and 305 mAh/g respectively. (Figure 8b) presents the Galvonastatic charge-discharge profile of Cu doped MoO_3 nanoparticles for 100 cycles and its first charge-discharge capacities are found to be 410 mAh/g and 415 mAh/g respectively. It is observed that very importantly compared to undoped MoO_3 nanoparticles Cu doped MoO_3 nanoparticles shows high specific capacity. From the charge-discharge profile it is observed that the capacity drastically decreased for second cycle and less reduction in capacity is also observed for higher cycles. The charge-discharge performances are enhanced for Cu doped MoO_3 nanoparticles compared to undoped MoO_3 nanoparticles since the band gap and the impedance for Cu doped MoO_3nanoparticles is less compared to undoped MoO_3 nanoparticles.

5. Conclusion

The synthesis of molybdenum oxide nanoparticles by green combustion method using *Terminalia catappa* plant extract. The Cu doped MoO_3 nanoparticles are synthesized by varying dopant concentration (2%, 4%, 6%, 8% and 10%) and then analysed by various structural, electrical and electrochemical performances are analysed. The XRD patterns confirms orthorhombic MoO_3 nanoparticles, also presents no CuO nanoparticles formation. The XRD studies of the material confirmed the crystal purity of the material, with the d-spacing for the (021) plane being found to be 41.98 nm. The SEM elemental mapping shows presence of Mo, O and Cu in synthesized Cu doped MoO_3 nanoparticles. The UV-Vis analysis shows the less band gap for 6% Cu doped MoO_3 nanoparticles. The specific capacity enhances for Cu doped MoO_3 compared to undoped MoO_3 and hence Cu doping plays very significant role in increasing the conductivity of the anode electrode material for Li-ion battery.

References

[1] Palit, S. and C.M. Hussain, Nanodevices applications and recent advancements in nanotechnology and the global pharmaceutical industry, in Nanomaterials in Diagnostic Tools and Devices. 2020, Elsevier. p. 395-415.

[2] Sagadevan, S. and M. Periasamy, Recent trends in nanobiosensors and their applications-a review. Rev Adv Mater Sci, 2014. 36(2014): p. 62-69.

[3] Patel, D.K., et al., Carbon nanotubes-based nanomaterials and their agricultural and biotechnological applications. Materials, 2020. 13(7): p. 1679.

[4] Pinto, B.F., et al., Effect of calcination temperature on the application of molybdenum trioxide acid catalyst: screening of substrates for biodiesel production. Fuel, 2019. 239: p. 290-296.

[5] Maduraiveeran, G., M. Sasidharan, and W. Jin, Earth-abundant transition metal and metal oxide nanomaterials: Synthesis and electrochemical applications. Progress in Materials Science, 2019. 106: p. 100574.

[6] Schmitt, A.L., et al., Synthesis and applications of metal silicide nanowires. Journal of Materials Chemistry, 2010. 20(2): p. 223-235.

[7] Ambigadevi, J., et al., Recent developments in photocatalytic remediation of textile effluent using semiconductor based nanostructured catalyst: A review. Journal of Environmental Chemical Engineering, 2021. 9(1): p. 104881.

[8] Vela, N., et al., Removal of polycyclic aromatic hydrocarbons (PAHs) from groundwater by heterogeneous photocatalysis under natural sunlight. Journal of Photochemistry and Photobiology A: Chemistry, 2012. 232: p. 32-40.

[9] Dong, R., et al., Enhanced supercapacitor performance of Mn3O4 nanocrystals by doping transition-metal ions. ACS applied materials & interfaces, 2013. 5(19): p. 9508-9516.

[10] Ruan, J., et al., Nitrogen-doped hollow carbon nanospheres towards the application of potassium ion storage. Journal of Materials Chemistry A, 2019. 7(33): p. 19305-19315.

[11] Shewale, P.S. and K.-S. Yun, Surface modified Ni wire supported flexible asymmetric supercapacitor of Mn3O4//PEDOT-PSS-MWCNT and its solar charging for self-powered Cu-doped ZnO nanorods-based UV photodetector. Journal of Alloys and Compounds, 2022. 911: p. 164939.

[12] Ahmad, S., et al., Sol-gel synthesis of nanostructured ZnO/SrZnO2 with boosted antibacterial and photocatalytic activity. Ceramics International, 2022. 48(2): p. 2394-2405.

[13] Letifi, H., et al., High efficient and cost effective titanium doped tin dioxide based photocatalysts synthesized via co-precipitation approach. Catalysts, 2021. 11(7): p. 803.

[14] Song, D., et al., Advancing recycling of spent lithium-ion batteries: from green chemistry to circular economy. Energy Storage Materials, 2023: p. 102870.

[15] Schofield, K., Combustion emissions: formation, reaction, and removal of trace metals in combustion products. 2020: Academic Press.

[16] Rammal, M.B. and S. Omanovic, Synthesis and characterization of NiO, MoO3, and NiMoO4 nanostructures through a green, facile method and their potential use as electrocatalysts for water splitting. Materials Chemistry and Physics, 2020. 255: p. 123570.

[17] Aggrey, P., et al., On the diatomite-based nanostructure-preserving material synthesis for energy applications. RSC advances, 2021. 11(51): p. 31884-31922.

[18] Dhenadhayalan, N., K.C. Lin, and T.A. Saleh, Recent advances in functionalized carbon dots toward the design of efficient materials for sensing and catalysis applications. Small, 2020. 16(1): p. 1905767.

[19] Rathod, S.B., et al., Preparation, characterization and catalytic activity of MoO3/CeO2–ZrO2 solid heterogeneous catalyst for the synthesis of β-enaminones. Arabian Journal of Chemistry, 2014. 7(3): p. 253-260.

[20] Nazri, G.-A. and C. Julien, Far-infrared and Raman studies of orthorhombic MoO3 single crystal. Solid State Ionics, 1992. 53: p. 376-382.

[21] Shakir, I., et al., MoO 3-MWCNT nanocomposite photocatalyst with control of light-harvesting under visible light and natural sunlight irradiation. Journal of Materials Chemistry, 2012. 22(38): p. 20549-20553.

[22] Patil, S.B., et al., High capacity MoO 3/rGO nanocomposite anode for lithium ion batteries: an intuition into the conversion mechanism of MoO 3. New Journal of Chemistry, 2018. 42(23): p. 18569-18577.

[23] Pham, T.-T., S.G. Kang, and E.W. Shin, Optical and structural properties of Mo-doped NiTiO3 materials synthesized via modified Pechini methods. Applied Surface Science, 2017. 411: p. 18-26.

[24] Sen, S.K., et al., Dy-doped MoO3 nanobelts synthesized via hydrothermal route: Influence of Dy contents on the structural, morphological and optical properties. Journal of Alloys and Compounds, 2021. 876: p. 160070.

[25] LIMA DA SILVA, A., et al., Synthesis of MoO 3 by Pilot Scale Combustion Reaction: Evaluation in Biodiesel Production from Residual Oil. Available at SSRN 3981557.

[26] Wang, J., M. Song, and H.J. Seo, Luminescence and energy transfer in BaY2 (MoO4) 4: Tb3+, Eu3+ phosphors and bifunctional applications in thermometry and light emitting diodes. Journal of Luminescence, 2020. 222: p. 117185.

[27] Kaushik, B., et al., Magnetically separable type-II semiconductor based ZnO/MoO 3 photocatalyst: a proficient system for heteroarenes arylation and rhodamine B degradation under visible light. New Journal of Chemistry, 2022. 46(18): p. 8478-8488.

[28] Zhao, J., C. Chen, and W. Ma, Photocatalytic degradation of organic pollutants under visible light irradiation. Topics in catalysis, 2005. 35: p. 269-278.

[29] Kamoun, O., et al., Synthesis and characterization of highly photocatalytic active Ce and Cu Co-doped novel spray pyrolysis developed MoO3 films for photocatalytic degradation of eosin-Y dye. Coatings, 2022. 12(6): p. 823.

[30] Boumediene, M., et al., Effects of pH and ionic strength on methylene blue removal from synthetic aqueous solutions by sorption onto orange peel and desorption study. J. Mater. Environ. Sci, 2018. 9(6): p. 1700-1711.

[31] Fil, B.A., C. Özmetin, and M. Korkmaz, Cationic dye (methylene blue) removal from aqueous solution by montmorillonite. 2012.

[32] Humayun, M., C. Wang, and W. Luo, Recent progress in the synthesis and applications of composite photocatalysts: a critical review. Small Methods, 2022. 6(2): p. 2101395.

[33] Prakash, K. and S. Karuthapandian, Construction of novel metal-free graphene oxide/graphitic carbon nitride nanohybrids: a 2D–2D amalgamation for the effective

dedyeing of waste water. Journal of Inorganic and Organometallic Polymers and Materials, 2021. 31: p. 716-730.

[34] De-Nasri, S.J., et al., Quantification of hydroxyl radicals in photocatalysis and acoustic cavitation: Utility of coumarin as a chemical probe. Chemical Engineering Journal, 2021. 420: p. 127560.

Citation: Harini R, Sunil T D, Kunal Roy, Dinesh Rangappa, G. Nagaraju. (2025). Development of MoO3 and Cu doped MoO3 Nanoparticles and its computational analysis for Lithium ion battery as anode electrode materials for energy storage applications. International Journal of Electronics and Instrumentation Engineering (IJEIE), 3(1), 7–23.

Abstract Link: https://iaeme.com/Home/article_id/IJEIE_03_01_002

Article Link:
https://iaeme.com/MasterAdmin/Journal_uploads/IJEIE/VOLUME_3_ISSUE_1/IJEIE_03_01_002.pdf

✉ **editor@iaeme.com**